Histone dynamics within the nucleosome octamer play a critical role in SNF2h-mediated nucleosome sliding

Nathan Gamarra[1,2], Geeta J. Narlikar[1]*

*Corresponding author: geeta.narlikar@ucsf.edu

[1]Department of Biochemistry and Biophysics, University of California, San Francisco, San Francisco, United States

[2]TETRAD Graduate Program, University of California, San Francisco, San Francisco, United States

Arising from: Yan et al. (2019) Nature Structure and Molecular Biology https://doi.org/10.1038/s41594-019-0199-9

Abstract

Elucidating the mechanisms by which ATP-dependent chromatin remodeling enzymes disrupt nucleosome structure is essential to understanding how chromatin states are established and maintained. A key finding informing remodeler mechanism is the observation that the dynamics of protein residues buried within the histone core of the nucleosome are required by specific remodelers to mobilize the nucleosome[1]. Recently, a study obtaining cryo-electron microscopy (cryo-EM) structures of remodeler-nucleosome complexes failed to observe stable conformational rearrangements in the histone octamer[2]. The authors of this study also failed to replicate the finding that site-specifically restraining histone dynamics inhibits nucleosome sliding by ISWI-family remodelers[2]. In contrast, a recent cryo-EM structure detected asymmetric histone dynamics in an ISWI-nucleosome complex[3]. Here, using two different protocols, we replicate the original finding in Sinha et al.[1] that dynamics within the histone core are required for nucleosome sliding by the human ISWI remodeler, SNF2h. These results firmly establish histone dynamics as an essential feature of ISWI-mediated nucleosome sliding and highlight the care required in designing and performing biochemical experiments investigating nucleosome dynamics.

Results and Discussion

In previous work, dynamics in the histone core were demonstrated to be functionally important for nucleosome sliding by SNF2h using site-specific disulfide crosslinks

engineered in otherwise cysteine-free histones[1]. These crosslinks inhibited nucleosome sliding by SNF2h, suggesting that inhibition of sliding was due to restraining histone octamer dynamics. To minimize any potential damage to the nucleosome that could influence the experimental results, oxidation reactions for generating the disulfide bond were carried out in the absence of metal catalysts, which can generate free radicals that may create non-specific damage[4].

In contrast, Yan et al.[2] reported that restraining histone dynamics using single H3-H4 crosslinks (H3L82C-H4V81C called sCX2) from Sinha et al.[1] did not specifically impact nucleosome sliding by SNF2h. Yan et al. first generated sCX2 crosslinks in the background of WT Xenopus laevis octamer, which bear an endogenous cysteine (H3C110) and found that sliding was unaffected. However, the presence of an additional reactive cysteine creates the possibility for multiple types of crosslinked species, complicating the interpretation of these results. Yan et al. also created sCX2 crosslinks in H3C110A octamer and, as in Sinha et al., found that SNF2h sliding activity was impaired, but to a much lesser extent than observed previously. Further, when the disulfide bond was apparently reduced by adding 100mM DTT, sliding activity was not restored. Based on these results, Yan et al. suggested, "…that the loss of activity did not result from the disulfide bond but probably from non-specific oxidation damage to the nucleosome, which was prone to precipitate out of the solution under the condition of extensive oxidation. Prolonged treatment might have resulted in damage to the nucleosome and loss of the activity." However, the authors did not directly test for this possibility as they did not report any remodeling experiments with nucleosomes lacking the cysteine residues that had been subjected to the same oxidation protocol.

We therefore set out to directly test the possibility raised by Yan et al. of non-specific oxidative damage to the histone octamer and to determine whether any differences in the protocols used to generate crosslinked nucleosomes could explain the discrepancies between the two studies. Unlike in Sinha et al., Yan et al. used copper phenanthroline (CuPhe), a harsh oxidizing agent which generates free radicals that may create non-specific oxidative damage[4]. We first hypothesized that non-specific oxidative damage by CuPhe could account for the discrepancy. To test for this possibility, we assembled nucleosomes with Xenopus laevis H3C110A octamer that had been oxidized with CuPhe

(Supplemental figure 1A). No defects were seen in the remodeling of these nucleosomes when compared to the remodeling of nucleosomes assembled from untreated H3C110A octamers (Table 1, Figure 1A). This result indicates that non-specific oxidative damage to the octamer cannot explain the remodeling defects. Additionally, unlike as reported by Yan et al., we do not observe any histone precipitation in any of our oxidation protocols.

We then wondered whether the oxidation method may impact the crosslinking results only in the context of H3C110A sCX2 octamer. To test this possibility, we generated H3C110A sCX2 crosslinked nucleosomes using CuPhe or using oxidized glutathione (GSSG), a gentler oxidizing agent that does not generate free radicals and has been used previously to investigate nucleosome dynamics[5]. Oxidation with CuPhe went to near-completion as assessed by a non-reducing SDS-PAGE gel, while GSSG oxidation was less efficient (Supplemental figure 1A). A portion of each H3C110A sCX2 crosslinked octamer was then reduced by dialysis into high salt buffer containing 100mM DTT (Supplemental figure 1B). Nucleosomes were assembled with each oxidized and reduced octamer and subjected to remodeling by SNF2h (Figure 1B). H3C110A sCX2 nucleosomes assembled with CuPhe oxidized octamer were slowed in nucleosome sliding ~40-fold compared to reduced controls under saturating SNF2h conditions, while GSSG octamer slowed sliding ~15-fold (Figure 1C). The difference in quantitative effects between the two oxidation methods can be attributed to the different crosslinking efficiencies in each sample. Reduction of either type of oxidized octamer sample fully restored sliding activity in nucleosomes assembled from the respective octamers (Figure 1B-C). Similar results were obtained with sub-saturating concentrations of enzyme (Supplemental Figure 2). These results indicate that the sliding inhibition observed with nucleosomes assembled using the oxidized H3C110A sCX2 octamer is explained by the disulfide bond mediated restraint placed on histone dynamics.

The results that we describe above, (i) rule out the model put forth by Yan et al. of non-specific octamer oxidation causing inhibition of sliding; (ii) reproduce the large inhibitory effects seen by Sinha et al. when the H3L82C-H4V81C disulfide bond is formed in an H3C110A nucleosome; and (iii) show that the large defect is completely reversible

when the oxidized octamer is reduced prior to nucleosome assembly. These results are summarized in Table 1.

Yan et al. carried out their test for reversibility in a different manner than Sinha et al. While they carried out the forward reaction, namely oxidation in the context of an octamer (as Sinha et al. did), they carried out the reverse reaction, namely reduction in the context of a nucleosome. In our experience, reducing buried disulfides in the context of a fully assembled nucleosome has been very difficult and we reason this is because the disulfide cross-link becomes substantially less solvent accessible in a nucleosome compared to an octamer. However, to complete our analysis of the discrepancy between Sinha et al., and Yan et al., we decided to test the method used by Yan et al. In their method for reducing the disulfide bonds, Yan et al. treated the crosslinked nucleosomes with 100mM DTT at 37ºC for 1hr before initiating remodeling reactions. When we reduced crosslinked H3C110A sCX2 nucleosomes as in Yan et al., we found that sliding activity was not restored, consistent with their report (Supplemental Figure 3A). Further, Yan et al. showed that these conditions were sufficient to completely break the disulfide bond when assayed by non-reducing SDS-PAGE. However, we reasoned that if the sample was not buffer exchanged to remove excess DTT prior to denaturation in SDS-PAGE loading buffer, once-buried disulfides could become exposed and rapidly reduced by residual reducing agent when denatured by SDS. This would cause an overestimate of the degree of reduction on the SDS-PAGE gel. To test for this possibility, we reduced H3C110A sCX2 crosslinked nucleosomes with 100mM DTT for 1hr at 37ºC. Half of this sample was directly denatured and loaded on an SDS-PAGE gel while the other half was buffer exchanged to remove residual DTT prior to sample denaturation (Supplemental Figure 3B). Buffer exchanging prior to SDS-PAGE sample preparation increased the fraction of crosslinked histone (Supplemental Figure 3C). This cannot be explained by re-oxidation of the disulfide bond upon removal of reducing agent as we have found that the rate of natural oxidation is very slow (taking several days to weeks), and samples were treated with iodoacetamide prior to boiling to block disulfide bond formation prior to loading on the gel. As a result, it is likely that the apparent inability to reverse defects associated with crosslinking by Yan et al. may have been due to an inability to completely reverse crosslinking in fully assembled nucleosomes.

Importantly, our results do not invalidate the other conclusions presented in Yan et al. nor do they cast any doubt on the quality and accuracy of the structural data presented. The structures presented by Yan et al. represent only the fraction of states that can be reconstructed to high resolution. Lowly-populated or highly dynamic states would likely be lost during the averaging required for high resolution analysis. Consistent with this possibility, a recent cryo-EM study captured multiple stable ISWI-nucleosome states[3]. While the highest resolution structures showed no clear evidence of conformational dynamics, lower resolution structures showed local reduction in the cryo-EM density that overlap both with dynamic regions captured by NMR in Sinha et al., and with the crosslinked residues tested here and in Sinha et al. These results are consistent with SNF2h promoting the formation of an ensemble of highly dynamic conformations that cannot be directly visualized by cryo-EM averaging. Thus, the absence of a stable deformed histone octamer in the cryo-EM density reported by Yan et al. is easily compatible with the finding that histone deformation is important for nucleosome sliding.

In summary, we are able to replicate the findings of Sinha et al. that restraining histone dynamics with disulfide crosslinks substantially interferes with SNF2h-mediated nucleosome sliding. We further show that this finding is robust to the method of crosslinking and cannot be explained by non-specific oxidative damage to the nucleosome. The inability to replicate this finding by Yan et al. is likely in part due to incomplete reduction of the disulfide bond in the context of the nucleosome.

Overall, our results are consistent with an important role for histone octamer plasticity during SNF2h-mediated nucleosome sliding. Further, these results underscore the importance of performing both oxidation and reduction reactions in the context of the histone octamer when attempting to generate or reverse crosslinks to investigate the role of histone dynamics.

Acknowledgements

We thank Kalyan Sinha for help generating the disulfide crosslinked nucleosome and Julia Tretyakova for preparing histones. We also thank Serena Sanulli, John Gross, Joseph Lobel, and Yifan Cheng for helpful feedback in preparing this manuscript and all members

of the Narlikar lab for helpful discussions. This work was supported by a grant from the NIH to GJN (R01GM073767) and an NSF predoctoral and UCSF discovery fellowship to NG.

References

1. Sinha K.K., Gross J.D., Narlikar G.J. Distortion of histone octamer core promotes nucleosome mobilization by a chromatin remodeler. Science. 355, eaa3761 (2017).
2. Yan L., Wu H., Li X. et al. Structures of the ISWI–nucleosome complex reveal a conserved mechanism of chromatin remodeling. Nat Struct Mol Biol 26, 258–266 (2019).
3. Armache J.P., Gamarra N., Johnson S.L., Leonard J.D., Wu S., Narlikar G.J., Cheng Y. Cryo-EM structures of remodeler-nucleosome intermediates suggest allosteric control through the nucleosome. eLife 18, e35322 (2019).
4. Maqsood S.R., Khan B., Bhat M.A., Dar T.A., Mir S.H. Targeting copper induced oxidative damage to proteins by ligation: a novel approach towards chelation therapy for oxidative stress disorders. New J. Chem 39, 2720-2727 (2015).
5. Sanulli S., Trnka M.J., Dharmarajan V., Tibble R.W., Pascal B.D., Burlingame A.L., Griffin P.R., Gross J.D., Narlikar G.J. HP1 reshapes nucleosome core to promote phase separation of heterochromatin. Nature 575, 390-394 (2019).
6. Luger K., Rechsteiner T.J., Richmond T.J. Preparation of nucleosome core particles from recombinant histones. Methods Enzymol. 304, 3-19 (1999).
7. Lowary P.T., Widom J. New DNA sequence rules for high affinity binding to histone octamer and sequence-directed nucleosome positioning. J Mol Biol. 276, 19-42 (1998).
8. Zhou C.Y., Narlikar G.J. Analysis of Nucleosome Sliding by ATP-Dependent Chromatin Remodeling Enzymes. Methods Enzymol. 573, 119-135 (2016).

Supplemental Methods

SNF2h was purified from E. coli as described previously[3]. Recombinant Xenopus laevis histones were expressed and purified from E. coli as previously described[6]. Cysteine mutant histones were purified in the presence of excess DTT. Mutant histones were also purified using only the gel-filtration step because cyanate formed in the urea buffers required for ion exchange reacts with the cysteine thiols[1]. Cy3-labeled nucleosome DNA was generated by PCR with HPLC-purified, labeled primers (IDT, Coralville, IA) and Phusion DNA polymerase using the strong, synthetic 601 nucleosome positioning sequence[7]. Nucleosome DNA was purified by native PAGE.

Histone octamer refolding was performed as described previously[3]. H3C110A sCX2 octamer was refolded in the presence of 10mM DTT to prevent disulfide formation. Refolded histone octamer and H2A/H2B dimer was purified by size exclusion chromatography with 10mM DTT. For oxidation, histone octamers and dimers were diluted to 5µM and ~200µL of sample was dialyzed twice into 1L high salt buffer without reducing agent (10mM HEPES pH 8.5, 2M NaCl, 1mM EDTA) each time overnight at 4°C.

For the CuPhe oxidation protocol, histone octamer and dimer was dialyzed overnight into 10 mM HEPES pH 7.25, 2 M NaCl. Histones were treated with 25µM Cu(II)SO4 and 100µM o-phenanthroline for 75 min at room temperature in the dark before being quenched with 10mM EDTA. Stocks of Cu(II)SO4 and o-phenanthroline used for oxidation were freshly dissolved in 10 mM HEPES pH 7.25, 2 M NaCl on the day of reaction. For the glutathione oxidation histones were mixed 4:1 by volume histone:glutathione buffer (250mM Tris pH 9.0, 2M NaCl, 7.5mM Oxidized Glutathione, 2.5mM Reduced Glutathione, 5mM Benzamidine, 0.5mM Leupeptin) at room temperature in the dark for 4 nights. To check the progress of oxidation, aliquots of each reaction were quenched with 50mM iodoacetamide and run on a non-reducing SDS-PAGE gel. Disappearance of the H3 and H4 bands and appearance of a higher molecular weight species was used to determine the progress of oxidation. Quantification of crosslinking was done by measuring the intensity of the H3-H4 crosslinked band and normalizing it to the intensity of the H2A/H2B band. After oxidation, histones were dialyzed into 1L of 10mM HEPES pH 8.5, 2M NaCl, 1mM EDTA overnight at 4°C.

To reduce oxidized histones, samples were dialyzed overnight into 10mM HEPES pH 8.5, 2M NaCl, 1mM EDTA, 100mM DTT at 4ºC. Reduced samples were checked using non-reducing SDS-PAGE. Loss of the high molecular weight species and reappearance of the H3 and H4 bands indicated complete reduction.

Nucleosomes were assembled using salt gradient dialysis and purified by glycerol gradient centrifugation as described previously[8]. Oxidized nucleosomes were assembled using buffers without reducing agent while reduced nucleosomes were assembled using buffers with 3mM TCEP.

All remodeling reactions were performed under single turnover conditions (enzyme in excess of nucleosomes) with saturating concentrations (1µM) or subsaturating (50nM) concentrations of SNF2h at 20°C with 15 nM nucleosomes, 12.5 mM HEPES pH 7.5, 2 mM Tris pH 7.5, 70 mM KCl, 5 mM ATP•MgCl2, 3 mM MgCl2 , 0.02% NP40, and ~3%(v/v) glycerol. Reactions were started with addition of enzyme and time points were quenched with excess ADP and plasmid DNA. Time points were then resolved by native PAGE (6% acrylamide, 0.5XTBE) and scanned on a Typhoon variable mode imager (GE Life Sciences, Pittsburgh, PA) by scanning for fluorescent labels. Gels were then quantified by densitometry using ImageJ. The fraction of nucleosomes end-positioned (i.e. unremodeled) at a given time point was determined by the ratio of fast-migrating nucleosomes to the total nucleosome intensity. This was fit to a single exponential decay using Prism 6 (GraphPad, La Jolla, CA).

Data availability

All relevant data are included in the paper and its supplementary information files. In addition, source data for the results presented are available from the corresponding author upon reasonable request.

Figure 1. Restraining nucleosome dynamics inhibits sliding by SNF2h regardless of method.

(A) Treatment of H3C110A histone octamer with CuPhe or GSSG does not affect nucleosome sliding by SNF2h. Left. Native gel sliding assay with saturating concentrations of SNF2h (1μM) and with or without saturating ATP and 15nM cy3-labeled nucleosomes using the indicated histone octamer. Nucleosomes were positioned at a DNA end with 60 bp of DNA flanking one side (0/60) using the Widom 601 positioning sequence. Time points were quenched with excess ADP and plasmid DNA and resolved on a 6% (29:1 bis) acrylamide gel. Higher migrating species are more centrally-positioned nucleosomes. Right. Quantification of the gel data plotted as the fraction of end-positioned nucleosomes over time. (B) Native gel remodeling assay as in (A) using nucleosomes assembled with oxidized or reduced H3C110A sCX2 octamers, compared to nucleosomes assembled with oxidized H3C110A octamers. Nucleosomes assembled with oxidized H3C110A sCX2 octamers are slid substantially slower than nucleosomes assembled with oxidized H3C110A octamers. This effect can be completely reversed by treatment of the oxidized H3C110A sCX2 octamer with reducing agent prior to nucleosome assembly. (C) Mean observed rate constants (k_{obs}) from 3 independent experiments. Error bars reflect the standard error of the mean (SEM).

Supplemental Figure 1. Preparation of crosslinked and reduced histone octamers

SDS-PAGE gels of Xenopus laevis of histones used to prepare nucleosomes in this study. (A) H3C110A histone octamer and H3C110A sCX2 (H3 L82C, H4 V81C) histone octamer oxidized using copper phenanthroline (CuPhe) or oxidized glutathione (GSSG). (B) The same samples used in (A) treated with 100mM DTT in order to reduce the disulfide bond.

Supplemental Figure 2. Histone dynamics are also important at sub-saturating concentrations of SNF2h

(A) Native gel remodeling assay with sub-saturating SNF2h (1μM), saturating ATP, and 15nM cy3-nucleosomes as in Figure 1. Nucleosomes assembled from oxidized H3C110A sCX2 octamers are remodeled substantially slower than nucleosomes assembled from untreated H3C110A octamers. Nucleosomes assembled from H3C110A sCX2 octamers that were first oxidized and then reduced are remodeled as fast as nucleosomes assembled from untreated H3C110A octamers. (B) Quantification of the gels in A. (C) Mean observed rate constants (k_{obs}) from 3 independent experiments. Error bars reflect the standard error of the mean (SEM). The asterisk denotes that the oxidized reaction condition was too slow to reliably quantify with the time points taken.

Supplemental Figure 3. Disulfide reduction is impaired in the context of the nucleosome

(A) Native gel remodeling assay with saturating SNF2h (1μM), saturating ATP, and 15nM cy3-nucleosomes as in Figure 1. Nucleosomes containing the oxidized sCX2 bonds were generated by oxidizing the H3C110A sCX2 octamer using CuPhe, and then assembling nucleosomes. Treatment of these nucleosomes with excess DTT as in Yan et al. fails to reverse the remodeling defect. (B) Scheme for the samples run in C. Nucleosomes treated with reducing agent were either boiled directly in non-reducing SDS-PAGE loading buffer or buffer exchanged to remove residual reducing agent before boiling in non-reducing SDS-PAGE loading buffer. (C) SDS-PAGE of samples treated as in B. Samples with reducing agent removed prior to running on the gel are more oxidized than with the reducing agent removed, suggesting that residual DTT in the nucleosome sample buffer could reduce the disulfide bond after incubation in SDS buffer. This could potentially explain the some of the discrepancies reported in Yan et al. Cross-linking ratio is quantified as the ratio of the intensity of the cross-linked H3-H4 band to the intensity of the combined H2A and H2B band.

Octamer used to assemble nucleosome	k_{obs}	
[SNF2h]	**1μM**	**50nM**
H3C110A Untreated	1.6±0.1 min^{-1}	0.03±0.01 min^{-1}
H3C110A CuPhe Oxidized	1.8±0.1 min^{-1}	Not Determined
H3C110A CuPhe Oxidized and then reduced	2.3±0.1 min^{-1}	Not Determined
H3C110A sCX2 CuPhe Oxidized	0.06±0.03 min^{-1}	Undetectable
H3C110A sCX2 CuPhe Oxidized and then reduced	2.5±0.4 min^{-1}	0.03±0.02 min^{-1}
H3C110A sCX2 GSSG Oxidized	0.14±.02 min^{-1}	Not Determined
H3C110A sCX2 GSSG Oxidized and then reduced	2.2±0.6 min^{-1}	Not Determined

Table 1. k_{obs} for nucleosome sliding of the given substrate at different concentrations of SNF2h

Table 1

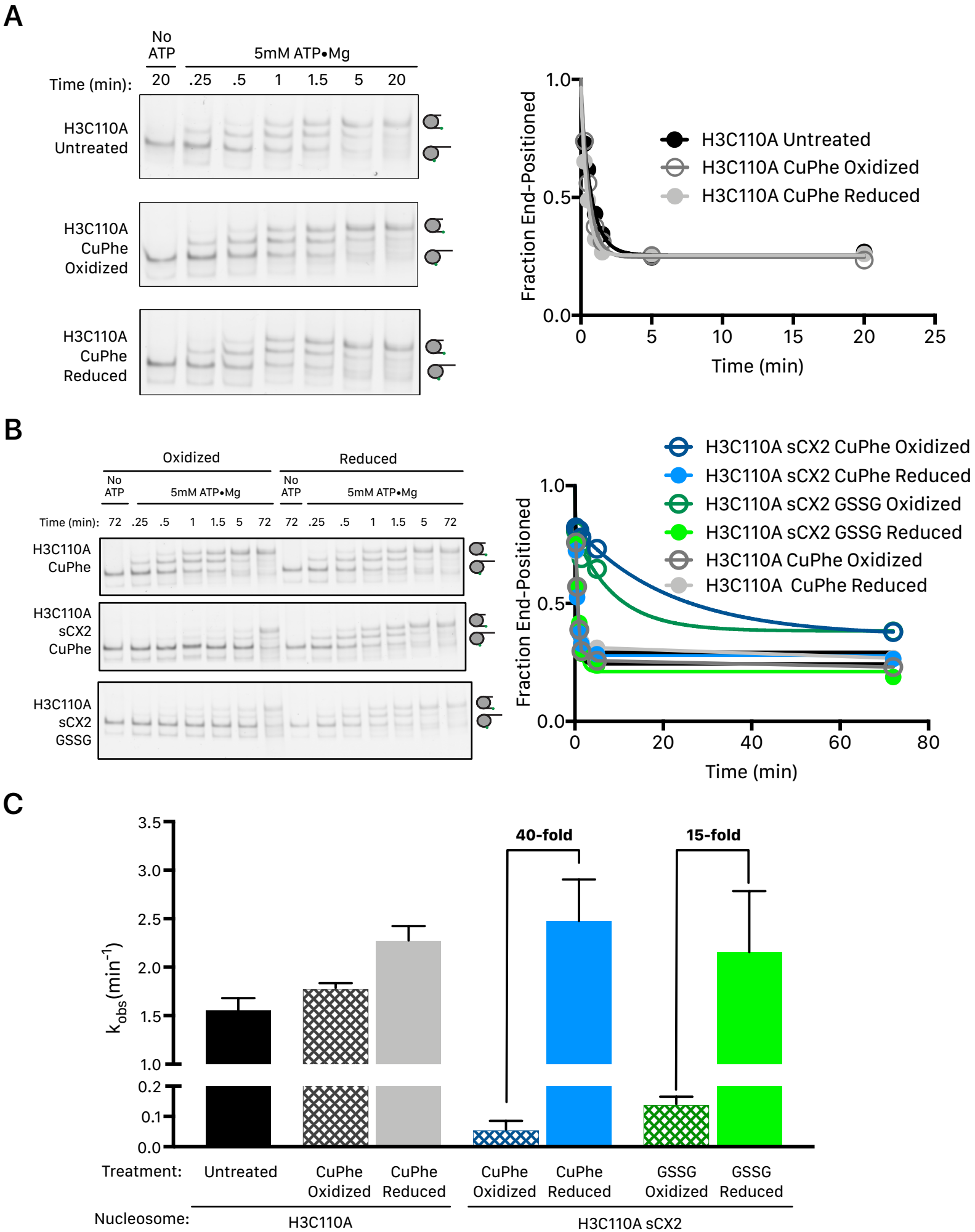
A
No ATP
5mM ATP•Mg
Time (min):
20
.25
.5
1
1.5
5
20
H3C110A Untreated
H3C110A CuPhe Oxidized
H3C110A CuPhe Reduced
Fraction End-Positioned
1.0
0.5
0.0
0
5
10
15
20
25
Time (min)
H3C110A Untreated
H3C110A CuPhe Oxidized
H3C110A CuPhe Reduced
B
Oxidized
Reduced
No ATP
5mM ATP•Mg
No ATP
5mM ATP•Mg
Time (min): 72 .25 .5 1 1.5 5 72 72 .25 .5 1 1.5 5 72
H3C110A CuPhe
H3C110A sCX2 CuPhe
H3C110A sCX2 GSSG
H3C110A sCX2 CuPhe Oxidized
H3C110A sCX2 CuPhe Reduced
H3C110A sCX2 GSSG Oxidized
H3C110A sCX2 GSSG Reduced
H3C110A CuPhe Oxidized
H3C110A CuPhe Reduced
Fraction End-Positioned
1.0
0.5
0.0
0
20
40
60
80
Time (min)
C
40-fold
15-fold
k_{obs} (min^{-1})
3.5
3.0
2.5
2.0
1.5
1.0
0.2
0.1
0.0
Treatment:
Untreated
CuPhe Oxidized
CuPhe Reduced
CuPhe Oxidized
CuPhe Reduced
GSSG Oxidized
GSSG Reduced
Nucleosome:
H3C110A
H3C110A sCX2

Figure 1

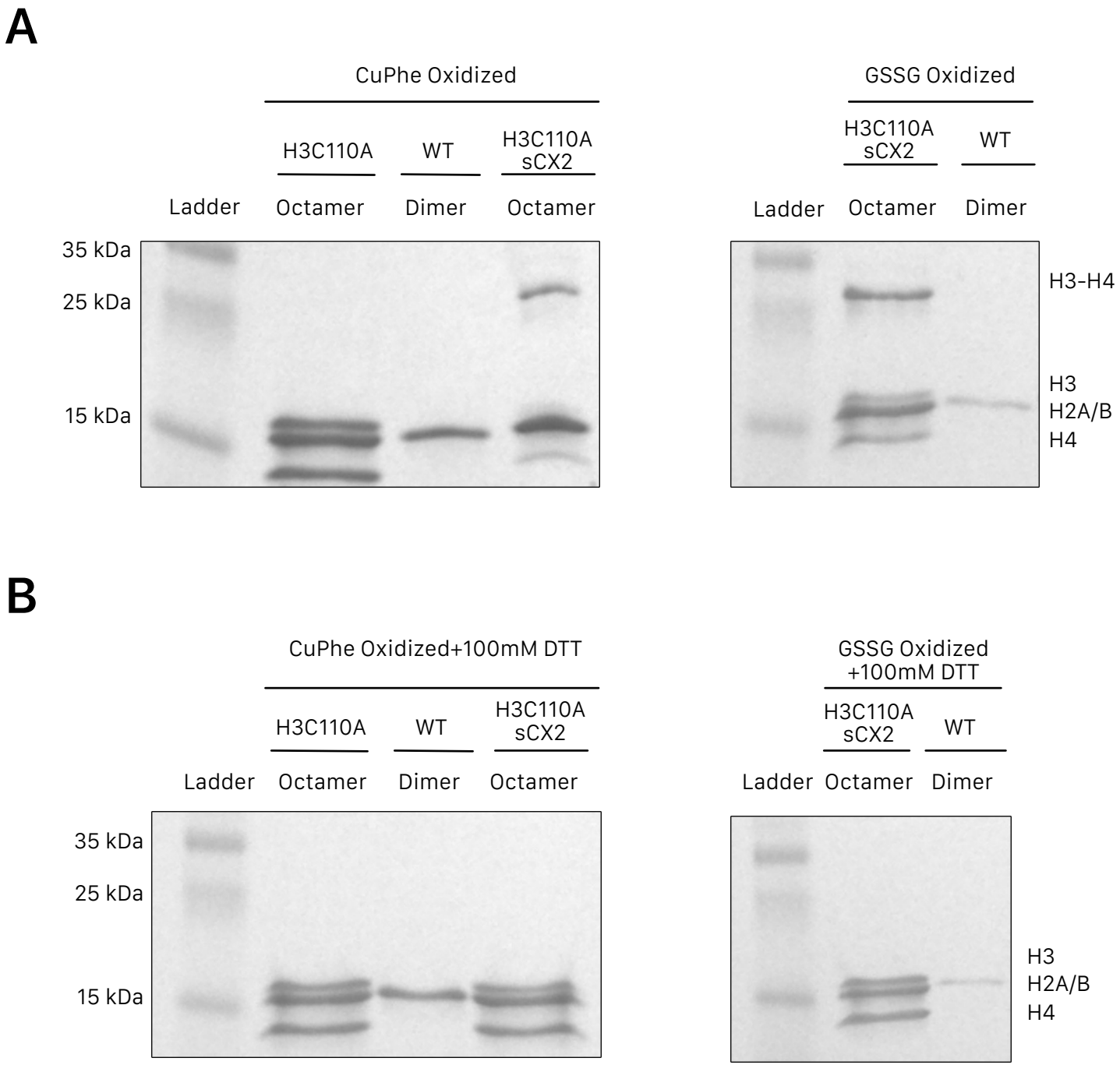

Supplemental Figure 1

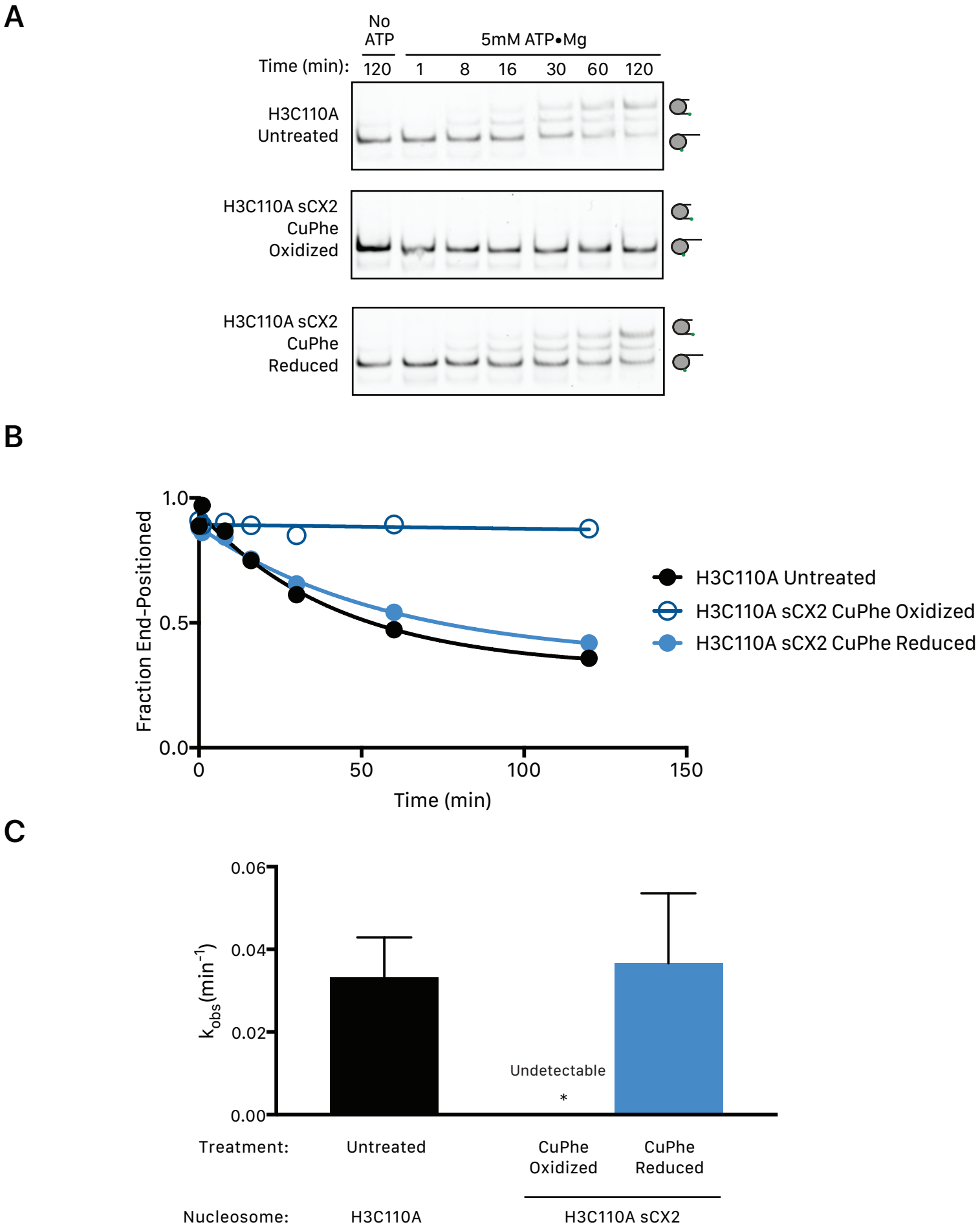

Supplemental Figure 2

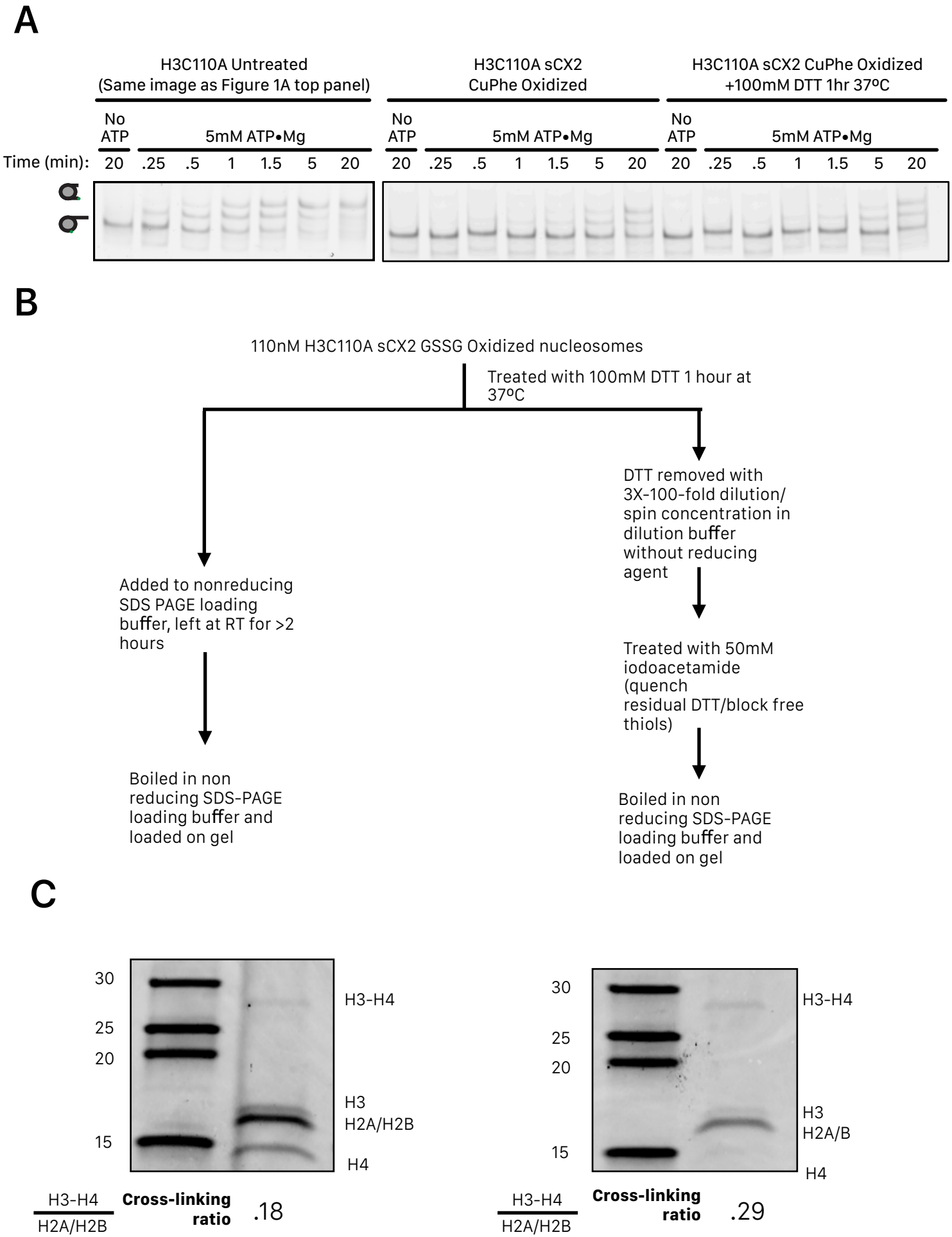

Supplemental Figure 3